Earth Surface Processes and Landforms
Earth Surf. Process. Landforms **26**, 307–318 (2001)

VISUAL CHARACTERIZATION TECHNIQUE FOR GRAVEL-COBBLE RIVER BED SURFACE SEDIMENTS; VALIDATION AND ENVIRONMENTAL APPLICATIONS CONTRIBUTION TO THE PROGRAMME OF CIRSA (CENTRE INTERUNIVERSITAIRE DE RECHERCHE SUR LE SAUMON ATLANTIQUE)

CHRISTIAN LATULIPPE,* MICHEL F. LAPOINTE AND TRACEY TALBOT
Department of Geography, McGill University, 805 Sherbrooke Street West, Montreal, Quebec, Canada, H3A 2K6

Received 14 July 1999; Revised 16 May 2000; Accepted 24 July 2000

ABSTRACT

This paper presents an evaluation of the feasibility and the reliability of a visual characterization technique for gravel–cobble river bed surface substrate. Based on principal axis regressions, using phi scale (ϕ), comparisons of visual estimation and grid sampling techniques show that useful predictive relations (R^2 = 0·78–0·88) exist between visual estimates of the surface d_{16}, d_{50} and d_{84} and estimates obtained for the same percentiles with the grid sampling technique. Comparisons of visual estimation and the surface-bulk sampling technique also indicate a predictive relation (R^2 = 0·70) between the d_{50} of the two methods. Trained operators can visually estimate gravel–cobble bed surface d_{16} to uncertainties of 41 per cent, d_{50} to 15 per cent and d_{84} to 11 per cent (for example, there is a 5·5 mm error on a d_{84} size of 50 mm). Furthermore, evidence shows that if operators are properly trained, a calibration relation for each percentile can be applied independently of operators. This visual characterization allows effective detailed mapping of spatial patterns in substrate size distribution along extensive reaches of gravel-bed rivers. The technique can be very useful in creating terrain models for various geomorphological, hydrological and biological applications such as the determination of entrainment thresholds, hydraulic roughness and substrate suitability for benthic insects or salmonid habitat.

KEY WORDS: visual characterization; surface substrate; sediment size and distribution; gravel-bed river; bed sampling technique

INTRODUCTION

The characterization of bed sediment calibre in a gravel-bed river involves spatial sampling difficulties due to lateral, longitudinal and depth variability of sediment size and distribution (Mosley and Tindale, 1985; Church *et al.*, 1987). The majority of existing sampling techniques (reviewed below) have been applied to spatially limited river forms such as riffles, pools and point bars (Milne, 1982; Payne and Lapointe, 1997). Nevertheless, these techniques are not optimized to describe with reasonable precision the lateral and longitudinal variability along long reaches of gravel-bed river, especially within a limited time span and the usual physical resources of a researcher. The usual way to achieve a spatial map of the sediment size distribution along a gravel-bed river has been to visually delimit the river bed into facies or areas whose surface grain size composition and distribution are approximately similar. This is followed by a characterization of the different areas by a surface sampling technique (Lisle and Madej, 1992; Sear, 1996; Buffington and Montgomery, 1999). This procedure, a form of stratified sampling, can be adequate, but it still relies on an initial visual delimitation of the boundaries of substrate facies in different areas. Because of the gradual nature of many facies transitions, this delimitation can be time consuming and relatively subjective in gravel-bed rivers. Furthermore, it has not been demonstrated that replication of this procedure by different operators can give consistent results.

---

* Correspondence to: C. Latulippe, Department of Geography, McGill University, 805 Sherbrooke Street West, Montreal, Quebec, Canada, H3A 2K6. E-mail: latulip@geog.mcgill.ca
Contract/grant sponsor: Centre Interuniversitaire de Recherche sur le Saumon Atlantique (CIRSA)

This study proposes a useful alternative visual technique to characterize the surface substrate (size and distribution) over an expanse of a gravel-bed river. The technique is quick, relatively precise and easy to apply in clear-water flows, even over long river reaches. It can also be easily coupled to grid data smoothing algorithms in common GIS packages to produce interpolated maps of substrate calibre information (example of which will be provided below). These maps can be useful to describe spatial patterns in stream habitat for various organisms as well as bed roughness and critical entrainment stress required in the development of two- or three-dimensional hydrodynamic or sediment transport models.

This paper is divided into four sections: (1) a brief review of bed sediment sampling techniques; (2) an explanation of the methodology and training protocol used for the visual estimation of a river bed surface sediment size distribution; (3) the error estimation linked to this technique and a comparison with common surface sampling techniques (grid sampling and surface-bulk sampling); and (4) a discussion of the applicability and some advantages of the proposed visual characterization technique.

SUBSTRATE SAMPLING REVIEW

A wide range of methods exist to characterize substrate. At the beginning of the 1950s, several researchers were interested in the size distribution of bed sediment in order to quantify the bed roughness of a channel flow. Indeed, Lane and Carlson (1953), while focusing on canal construction, developed a surface sampling technique to evaluate the Manning coefficient. This technique consists of extracting a thin surface layer of 1 m^2 area for sieve analysis. For similar reasons, Wolman (1954) developed a grid sampling technique, which involves setting a grid over the surface and picking up the particles immediately beneath each point on the grid. Usually, it is recommended that 100 particles be collected and their b-axis measured, which is the more representative axis to estimate diameter of an ellipsoidal particle (Koster *et al.*, 1980). Unlike the frequency-by-weight relations of volumetric sampling techniques, the Wolman grid techniques use frequency-by-number statistics (Church *et al.*, 1987). Kellerhals and Bray (1971) proposed conversion formulae to relate these various types of grain size statistics. Several variations exist of these basic techniques, such as the photographic technique (Adams, 1979) and the greased-block technique (Ettema, 1984).

In 1964, biologists interested in the gravel-size distribution in salmon spawning areas developed their own sampling technique using 'McNeil-type samplers' (McNeil and Ahnell, 1964). This method involves collecting sediment (from 6 to 15 kg) under water to a depth of 60 cm into the substrate. Walkotten (1973) developed another approach, called the 'freeze-core technique'. A hollow rod is inserted into the bed into which cooling liquid (carbon dioxin or nitrogen) is injected. This binds the particles surrounding the rod and allows them to be extracted for analysis. Rood and Church (1994) emphasized some weaknesses of these methods: the McNeil-type samplers may undersample the fine particle content and it is impossible to predetermine the volume of sediment for the freeze-core technique. Furthermore, individual samples by either technique may be too small to allow a statistically precise characterization of cobble/gravel substrate size distribution. Therefore, Rood and Church (1994) proposed a combination of the two techniques. This technique consists of burying a 20 cm diameter barrel in a bed to a depth of 30 cm, the maximum depth usually used by some salmonid for spawning (Devries, 1997), and into which the freeze-core technique is applied. This method has proven to be efficient to a water depth of 1·1 m and collects approximately 13·5 kg of sediments. Payne and Lapointe (1997) used a flow-isolation chamber for extracting large masses (100 kg) of substrate in a subaqueous environment.

METHODOLOGY OF THE VISUAL CHARACTERIZATION TECHNIQUE

The visual characterization technique for surface substrate proposed in this paper allows a rapid visual estimation of the surface grain size distribution of a 1 m^2 bed area (either emerged or submerged under clear water). Particles less than 2 mm in diameter are not taken into account in the visual estimation, consequently limiting the technique to gravel-bed rivers. This technique was developed and tested for moderately rounded sediments in an alluvial gravel–cobble river and has not been tested for highly imbricated, platy sediments and in systems dominated by boulders or clusters. The grain size range of the 1 m^2 area varied between 2 and 38 mm (d_{16}), 11 and 64 mm (d_{50}) and 24 and 115 mm (d_{84}). Additional studies are needed to validate this visual technique for other river environments.

Training protocol

Using a subaqueous grid sample technique, Wohl *et al.* (1996) noted that multiple operators can produce statistically different measures of d_{50} and d_{84}. Marcus *et al.* (1995) noted that the size estimate precision decreases when multiple operators with different bias pool their samples and suggested rigorous training to reduce this effect. To achieve statistically consistent results, operator training is necessary before carrying out visual grain size surveys. The operators are first trained to estimate visually the b-axis length of 200 particles (ranging in size from 5 to 160 mm) laid out on a table. After training, operators are usually capable of doing this to an accuracy of 15 per cent of diameter. An introduction is then given to the basic substrate surface sampling techniques (grid and surface-bulk sampling techniques). Operators are informed that in a spatially random or systematic sample of a bed surface (such as a grid sample), with data ranked by particle diameters, the d_{16}, d_{50} and d_{84} diameters correspond to those particle sizes such that 16, 50 and 84 per cent of the sampled bed area, respectively, is covered by particles smaller than the given size. Operators then attempt to visually estimate the d_{16}, d_{50} and d_{84} (in mm) of 20 different 1 m^2 areas of contrasting texture on the study gravel–cobble river system. Immediately after visual estimation, the operators apply the grid sampling technique on exactly the same area (with a 1 m^2 grid and by picking up 100 particles) to calculate the size of the percentile needed. The operators are then instructed to replace each rock in the exact position from which it was taken for measurement. This is immediately followed by a surface-bulk sampling technique, where the thickness of the surface layer on a 1 m^2 area is defined by the depth of the hole left by removing the largest rock (Church *et al.*, 1987). The surface layer is then entirely removed, mass is recorded and grains are sieved and weighed. The reliable estimates of the d_{16}, d_{50} and d_{84} of each 1 m^2 area based on accepted surface sampling techniques (grid sampling and surface-bulk sampling) are communicated to the operators immediately after they complete each of the sampling techniques. This allows the operators to further train and calibrate their visual estimations. This training protocol takes approximately two to three days.

ERROR ESTIMATION OF VISUAL CHARACTERIZATION TECHNIQUE

After this training, a study was conducted on 37 new sites using the same protocol. On these 1 m^2 sites, operators were asked to perform visual estimations of the d_{16}, d_{50} and d_{84}. To evaluate the reliability of the visual characterization technique, visual estimations of the d_{16}, d_{50} and d_{84} were compared to the results on the same area of the d_{16}, d_{50} and d_{84} given by the grid sampling and surface-bulk sampling. Principal axis regressions were used to analyse the relationship among various types of size estimates.

Comparisons between visual sampling and grid sampling technique

Three trained operators (S1, S2 and S3) completed visual estimations of the d_{16}, d_{50} and d_{84} on respectively 29, 21 and 18 of the 37 1 m^2 sites sampled. Typically, researchers will use the visual field estimate and convert these to equivalent grid sampling results, using a calibration relation developed for each visual estimator. Since all surface sampling techniques (visual, grid and surface-bulk) are subject to measurement error, a least squares simple linear regression cannot be used for purposes of calibration or prediction of one sampling technique to another. It has been suggested that when all variables are in the same units of measurement, the principal axis method provides a single axis to represent the trend between two variables (Mark and Church, 1977; Sokal and Rohlf, 1981).

Principal axis regressions were obtained for comparisons between the visual estimations of an operator and the results of a grid sampling for the same percentile. It should be noted that the data have been transformed from millimetres to a phi scale (Wentworth, 1922; Church *et al.*, 1987). Nine principal axis regression equations were derived, one for each operator and size percentile (Figure 1). Back transformed to millimetres,

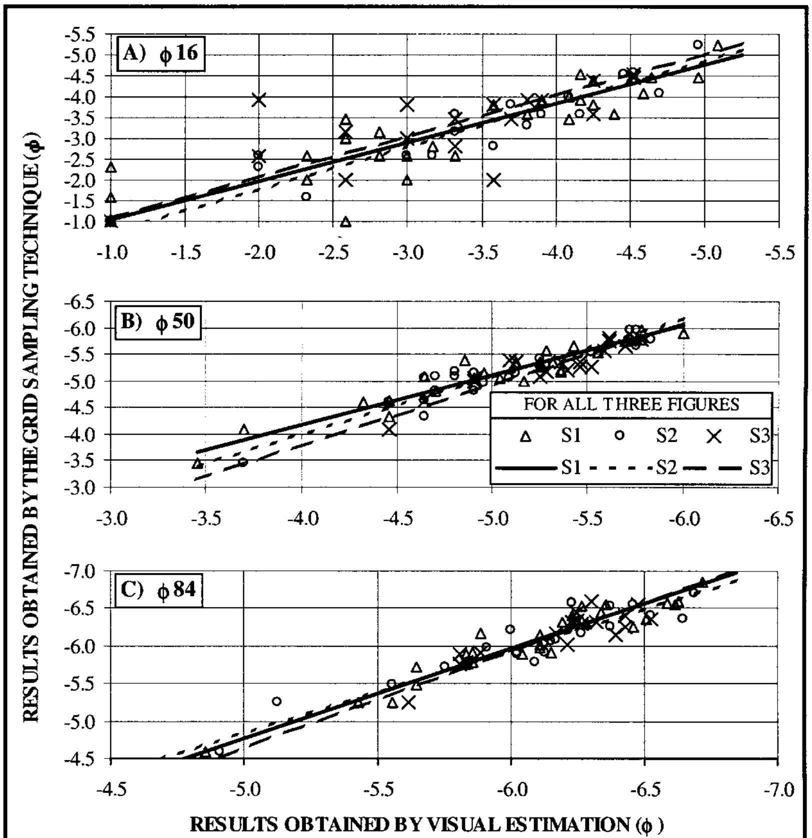

Combination			Correlation		Principal axis regression		Error
#	Samplers	Percentiles	n	R^2	b	a	SE
1	S1	ϕ16	29	0.746	0.937	-0.090	0.568
2	S2	ϕ16	21	0.863	1.026	0.277	0.403
3	S3	ϕ16	18	0.519	0.987	-0.089	0.731
4	S1	ϕ50	29	0.915	0.936	-0.421	0.172
5	S2	ϕ50	21	0.889	1.093	0.390	0.205
6	S3	ϕ50	18	0.812	1.159	0.862	0.194
7	S1	ϕ84	29	0.910	1.207	1.275	0.153
8	S2	ϕ84	21	0.878	1.107	0.700	0.179
9	S3	ϕ84	18	0.778	1.288	1.801	0.171

Figure 1. Relation between visual estimates of three different samplers and corresponding grid sampling results on 1 m^2 area, for three percentiles: (A) ϕ16; (B) ϕ50; (C) ϕ84

this yields error estimates expressed in percentages. This is consistent with having size uncertainties which scale with particle diameter. Note that standard errors in predicting the grid result from visual estimation (SE (vis-grid)) are larger for the d_{16} but relatively identical for d_{50} and d_{84} (Figure 1).

Slope and intercept comparisons (Scherrer, 1984; Zar, 1984) of the principal axis regression equations were conducted separately for each percentile (d_{16}, d_{50} and d_{84}), to determine if there is a significant difference in the trend of the visual to grid calibrations among operators. The analysis demonstrates that, for each percentile, the slope and the elevation given by the principal axis regression cannot be considered significantly different (at $\alpha = 0{\cdot}05$) among the operators. Therefore, data can be pooled for the three trained operators and useful predictive equations are obtained between visual estimates and grid sampling results for each percentile (Figure 2). Although different trained operators may have different bias, the calibration

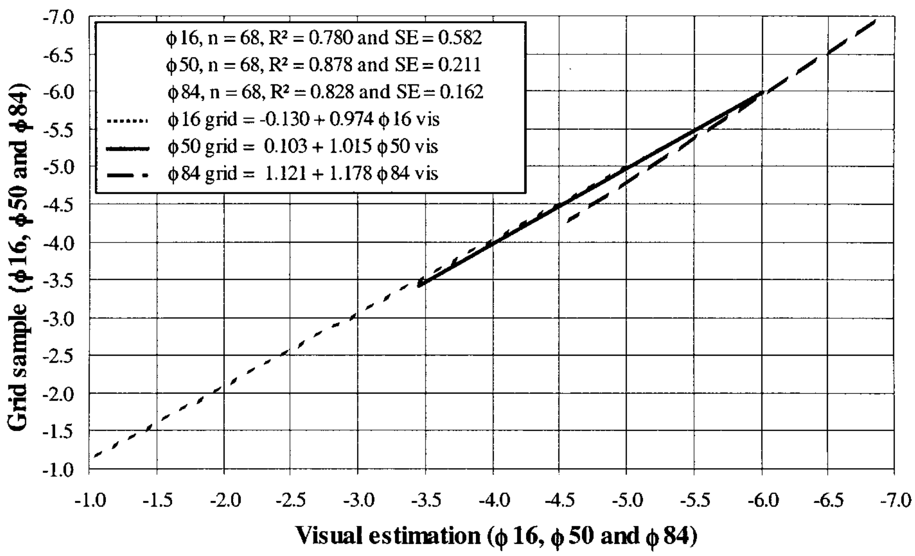

Figure 2. Comparison between visual estimations and grid sampling results for each percentile using pooled data of all samplers

equations for d_{16} and d_{50} of our three operators were not significantly different from the line of agreement. The SE (vis-grid) obtained by the pooled data demonstrates that the three operators can visually estimate bed surface ϕ_{16} to uncertainties of $0{\cdot}582\phi$, ϕ_{50} to $0{\cdot}211\phi$ and ϕ_{84} to $0{\cdot}162\phi$. Therefore, general calibration relations to transform visual estimates into equivalent grid sampling results for the study operators are given as follows:

$$\phi_{16\text{ grid}} = 0\cdot974\ \phi_{16\text{ vis}} - 0\cdot130 \text{ and SE (vis-grid)} = 0\cdot582$$

$$d_{16\text{ grid}} = 1\cdot094\ (d_{16\text{ vis}})^{0\cdot974} \text{ and SE (vis-grid) is approximately 41 per cent}$$

$$\phi_{50\text{ grid}} = 1\cdot015\ \phi_{50\text{ vis}} + 0\cdot103 \text{ and SE (vis-grid)} = 0\cdot211$$

$$d_{50\text{ grid}} = 0\cdot931\ (d_{50\text{ vis}})^{1\cdot015} \text{ and SE (vis-grid) is approximately 15 per cent}$$

$$\phi_{84\text{ grid}} = 1\cdot178\ \phi_{84\text{ vis}} + 1\cdot121 \text{ and SE (vis-grid)} = 0\cdot162$$

$$d_{84\text{ grid}} = 0\cdot460\ (d_{84\text{ vis}})^{1\cdot178} \text{ and SE (vis-grid) is approximately 11 per cent}$$

In general, the best candidates for visual characterization would be those with consistent (or zero) bias and smallest possible random error (based on standard error statistics)

Relation between visual sampling and surface-bulk sampling technique

The complex relation between a surface count sample (such as a grid sampling) and a bulk sample of the armour layer has been investigated theoretically and experimentally (Kellerhals and Bray, 1971; Hoey and Ferguson, 1994). In this section, visual estimates were compared to surface-bulk sampling results for each percentile. Using the same analysis as the previous section, comparisons of the principal axis regressions indicate that the slope and intercept of the calibration equation cannot be considered different (at $\alpha = 0{\cdot}05$) for the d_{50} only, among the operators (Figure 3). The uncertainties in the calibration of the visual estimate to the

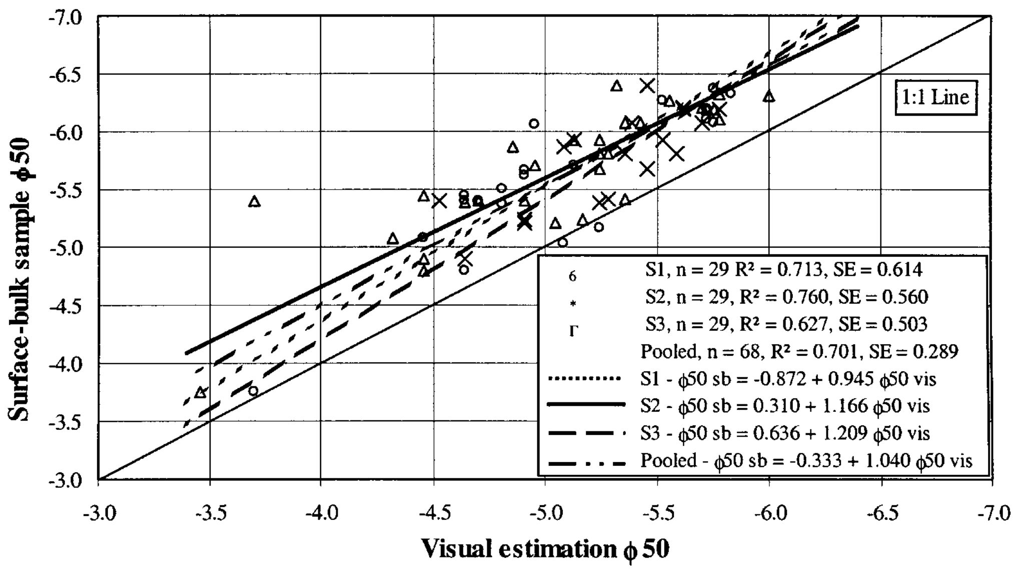

Figure 3. Comparison between visual estimations and grid sampling results for each percentile using pooled data of all samplers

surface-bulk sampling (SEϕ_{50} (vis-sb) = 0·289ϕ or approximately 20 per cent of d_{50}) are larger then the imprecision in calibrating visual estimates to grid sampling for the same percentile (0·21ϕ or 15 per cent of d_{50}).

In summary, calibration between visual estimations and grid sampling results for the three percentiles studied are operator independent, but less precise for d_{16} than coarser percentiles. The relation between the visual and surface-bulk technique is significantly different from line 1:1 and only operator independent for d_{50} percentile. The principal axis regressions on Figure 3 reveal that visual sampling technique tends to underestimate the size of the d_{50} with respect to surface-bulk sampling results. The latter result is to be expected. This is logically consistent with Hoey and Ferguson's (1994) findings that grid-based d_{50} estimates of the surface layer tend to be systematically smaller than bulk d_{50} values. This also appears to be inconsistent with the Kellerhals and Bray (1971) prediction that grid sampling is equivalent to bulk sieve analysis.

APPLICABILITY AND ADVANTAGES OF THE VISUAL CHARACTERIZATION TECHNIQUE

Percentiles of the grain size distribution can be used to estimate several geomorphological, hydrological or biological variables, such as bed roughness (Limerinos, 1970; Bray, 1979; Hey, 1979), critical shear stress for entrainment (Chang, 1992; Simons and Sentürk, 1992) and related bed material transport predictions (Meyer-Peter and Muller, 1948; Einstein, 1950; Parker, 1990). Bed surface d_{16}, d_{50} and d_{84} can also be useful to characterize visual estimates of riffle zone gravels for salmonid reproduction (Kondolf and Wolman, 1993; Moir *et al.*, 1996) as well as habitat suitability for various fishes (Morantz *et al.*, 1987; Heggenes, 1996; Heggenes *et al.*, 1996) or benthic macroinvertebrates (Muotka *et al.*, 1996).

The advantage of the visual characterization technique becomes obvious when estimating grain size distributions along several kilometre-long reaches of gravel-bed rivers, where the lateral and longitudinal sedimentological variability is important. Properly trained and calibrated operators require only a few seconds to evaluate grain size percentiles of the bed surface over 1 m^2 area and hundreds of such georeferenced estimates can be easily done in a reach. Visual estimates can be calibrated against other well known river bed surface sediment sampling techniques, such as grid and surface-bulk sampling, with an acceptable level of precision for many applications.

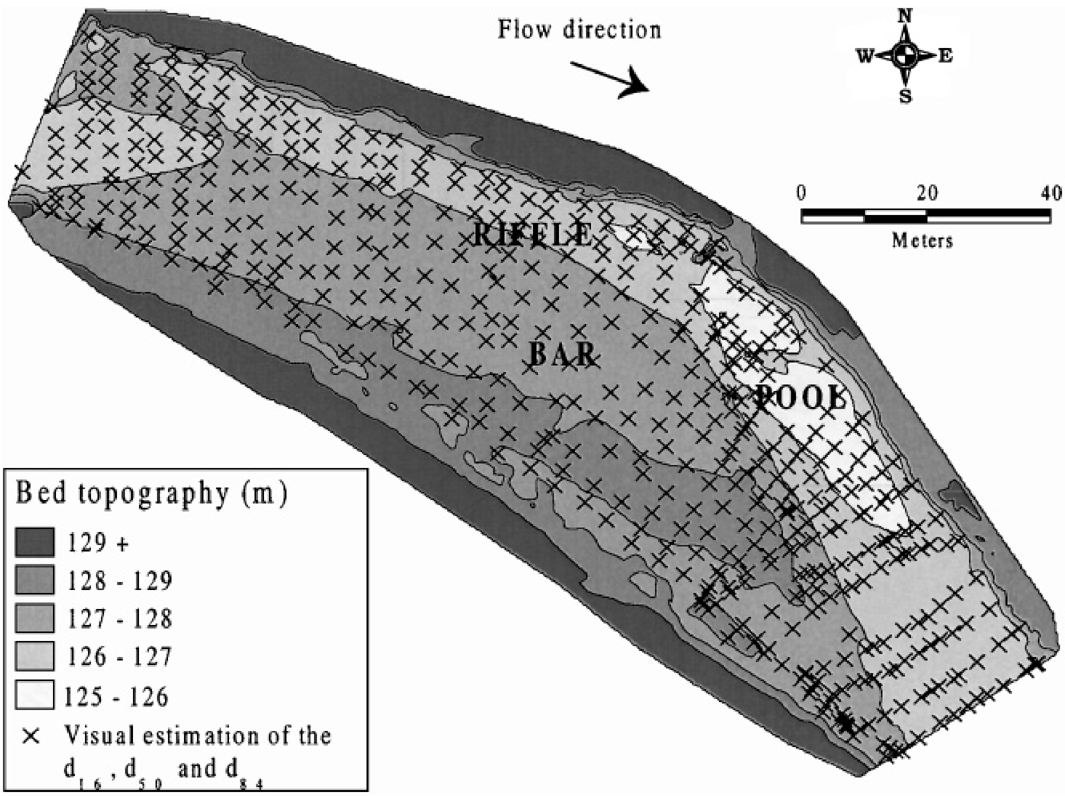

Figure 4. Visual estimation of bed-surface sediment on a 100 m reach of the Sainte-Marguerite River

The method developed in this paper was applied on a 4 km section of the Sainte-Marguerite River (Canada). A description of the river bed substrate with the visual estimation technique was integrated into a topographic survey of the river done with a total station. At almost every topographic sounding point, d_{16}, d_{50} and d_{84} were estimated visually and input in the georeference database. A dense coverage of visual estimations (Figure 4) can be made within a reach to estimate variables linked to the sediment size and distribution in a series of geomorphological and biological applications.

Sediment size descriptors

The visual characterization technique can be applied to derive and map sediment size and distribution statistics (Inman, 1952; Kondolf and Wolman, 1993), often used in stream ecological characterization. After conversion of the visual estimation to an equivalent grid sampling value (in millimetres), the geometric mean surface substrate size at various points in a river reach can be interpolated using $[(\phi_{84} + \phi_{16}) / 2]$ at every visual sampling point (Figure 5). Using this technique, the longitudinal and lateral variability of mean surface grain size becomes apparent. Based on the uncertainties of d_{16} and d_{84}, the standard error of the geometric mean calculated is $0{\cdot}37\phi$ or approximately 26 per cent. This error is not significant, when producing an interpolated map of geometric mean with a phi size contour interval. The sorting index (i.e. the degree of local heterogeneity at the bed surface) defined as $[(\phi_{84} - \phi_{16}) / 2]$ is mapped in Figure 6. The standard error of the sorting index equals $0{\cdot}21\phi$ or approximately 14 per cent. For the reach studied, riffle composed of very coarse gravel has a notably large area with high homogeneity (sorting index $\approx$2), presumably an indication of sorting by transport over many metres under a fairly uniform bed stress regime. The point bar tends firstly to fine downstream from very coarse gravel to granules and secondly to be relatively homogeneous, excepted at

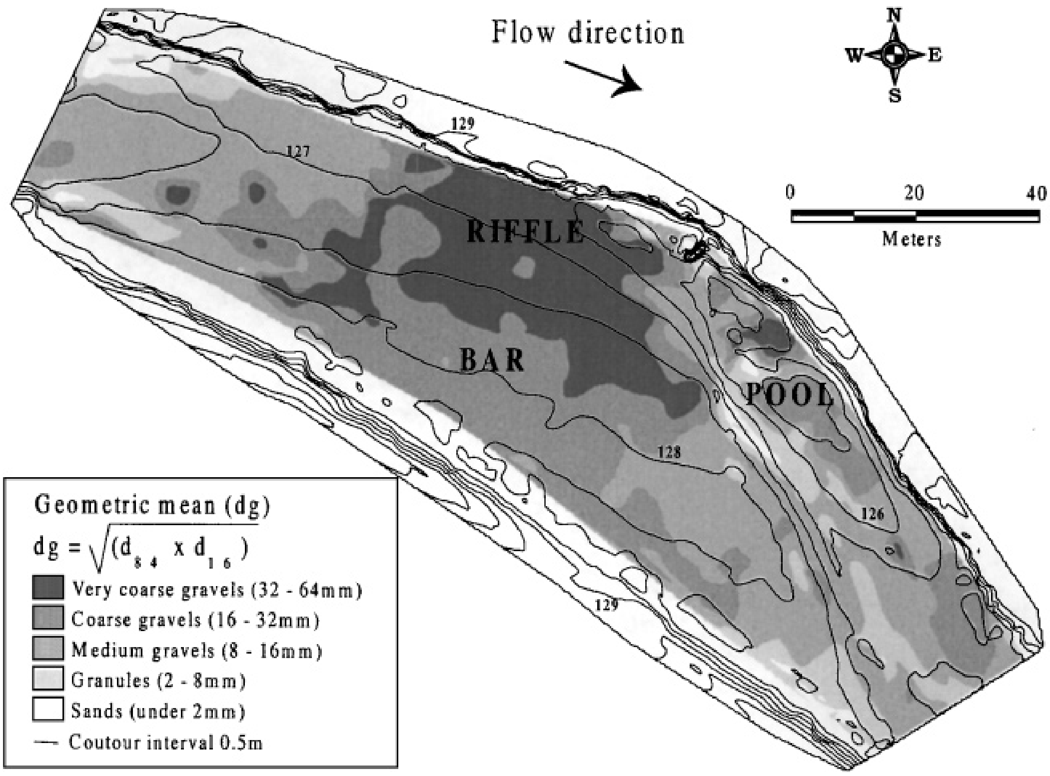

Figure 5. Geometric mean calculated using the visual characterization technique.

its tail where sorting index increases. The pool is composed of gravel-size particles and is very heterogeneous.

Bed roughness, shear stress and critical shear stress estimation

The percentiles estimated with the visual sampling technique can be used as input to bed roughness equations based on surface percentiles, yielding a dense field of estimated bed roughness values. A map of the bed roughness, based on the Manning–Strickler formula (Richards, 1982), where $n = 0{\cdot}0151\ d_{50}{}^{1/6}$, is presented in Figure 7 and takes into account the lateral and longitudinal variability of sediment textures. The percentages of error of the Manning–Strickler coefficient using the visual estimation converted into grid sampling value or into surface-bulk sampling value are 2·4 and 3·3 per cent respectively. Therefore, only the fourth decimal of the Manning–Strickler coefficient is affected by grain size uncertainty. Terrain maps such as Figure 7 have the potential to improve the accuracy of two- or three-dimensional hydrodynamic simulations.

Shear stress and critical shear stress maps

The relation between applied bed shear stress (τ_o) and critical shear stress for entrainment (τ_c) is used to model sediment transport in rivers. The depth-average velocity method (Wilcock, 1996) or the near-bed velocity method (Ippen and Drinker, 1962) are often used to calculate shear stresses on a river bed. These methods require measurements of flow velocity, water depth and estimates of local bed roughness length (z_0). Bed roughness length can be computed by several formulae based primarily on d_{84} or d_{90} (Hey; 1979; Whiting and Dietrich, 1990; Wiberg and Smith, 1991; Wilcock, 1996). Local shear stress can be estimated by combining (1) depth average velocity method (Wilcock, 1996), (2) Whiting and Dietrich (1990) formula to

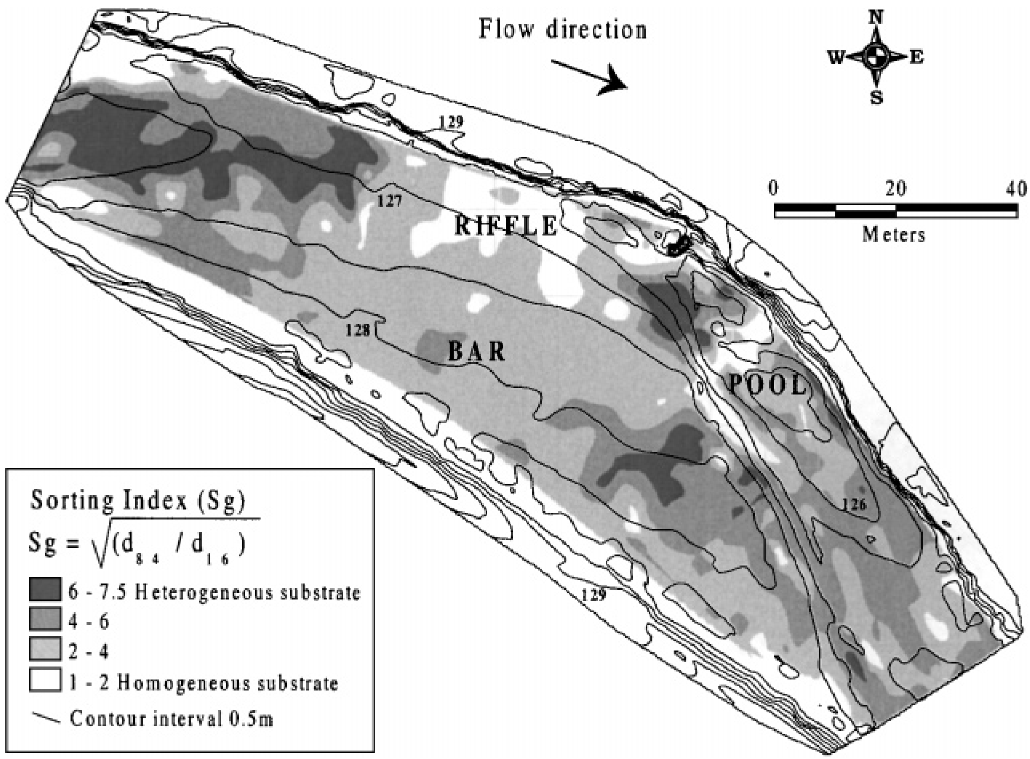

Figure 6. Sorting index of the surface substrate size calculated using the visual characterization technique

calculate z_0 and (3) visual technique to estimate d_{84}. Given the form of the log law of the wall (Dingman, 1984), the component of the error in τ_o due to the uncertainty in d_{84} from the visual estimate depends essentially on the ratio of depth to d_{84} (Figure 8). Excluding the effects of the error on water depth and flow velocity calculations, the error on τ_o induced by the visual technique is under 7 per cent for depth greater than ten times d_{84}. Since the critical shear stress (τ_c) is proportional to surface layer d_{50} (Dingman, 1984) their percentage errors will be of the same magnitude (i.e. 15 per cent). An example of sediment transport calculation is given to illustrate the propagation of errors in this case. The analysis below of course only accounts for the error directly related to the input of uncertain grain size variables in existing transport models. Other important errors in model specification also need to be considered.

On a uniform bed surface area with d_{50} of 32 mm, water depth of 1 m, mean velocity of $1{\cdot}5$ m s^{-1}, the shear stress computed by depth average velocity method (Wilcock, 1996) with z_0 based on local d_{84} of 64 mm is $21{\cdot}93 \pm 1{\cdot}19$ Pa. The transport rate estimated by Einstein–Brown formula (Chang, 1992) is $16{\cdot}2$ g ms^{-1}. Given the uncertainties on τ_o (5·4 per cent) and d_{50} or τ_c (15 per cent) involved by using the visual characterization technique, the sediment transport rate estimation varies between 3·0 and 68·8 g ms^{-1}. These uncertainties remain considerable. However, taking into account the spatial variability of grain size in a sediment transport model can yield useful insights into lateral and longitudinal variability of sediment transport rate, a major issue in modelling gravel-bed river evolution.

CONCLUSION

The visual surface substrate characterization technique proposed in this paper can efficiently and rapidly provide estimates of the d_{16}, d_{50} and d_{84} over a 1 m^2 bed surface area and can be applied on both submerged and emergent sites. The technique is relatively simple, but requires adequate operator training for

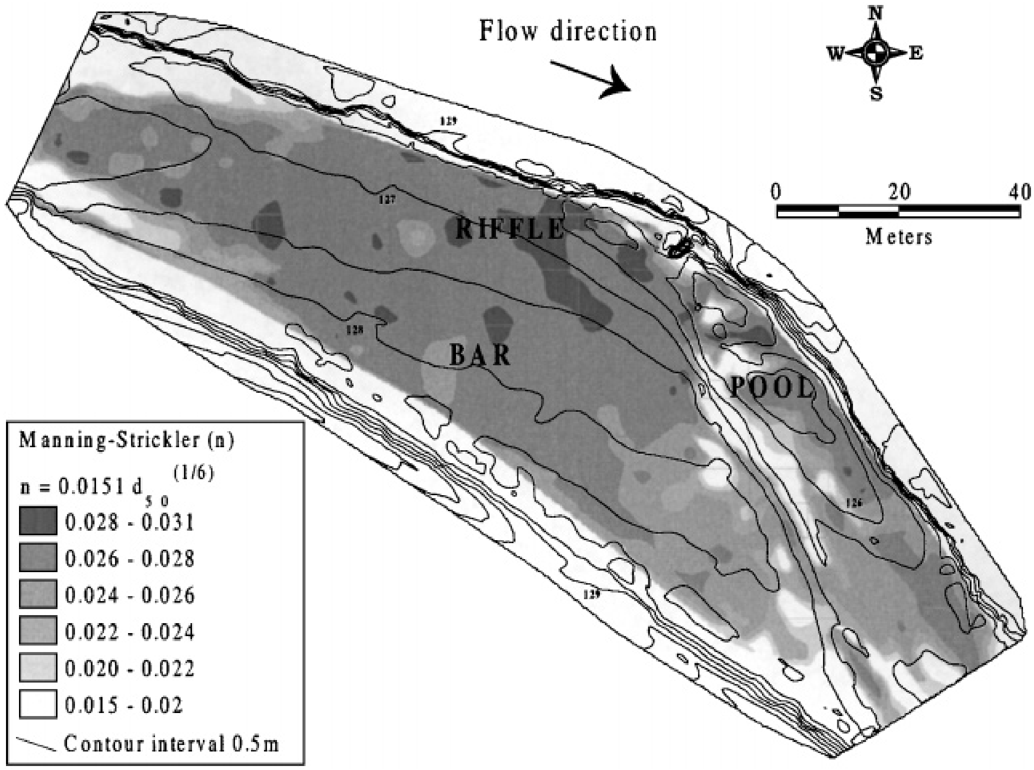

Figure 7. Map of bed roughness using the d_{50} obtained by the visual characterization technique and Manning–Strickler formula

reproducibility. Trained operators can develop individual calibration equations to relate their visual estimates of the d_{16}, d_{50} and d_{84} to results for identical percentiles obtained by grid sampling technique. Because this technique is relatively fast and reasonably precise, high-density local estimates can be gathered on a river bed and the important lateral and longitudinal variability of sediment size distribution of a gravel-bed river can be characterized more accurately.

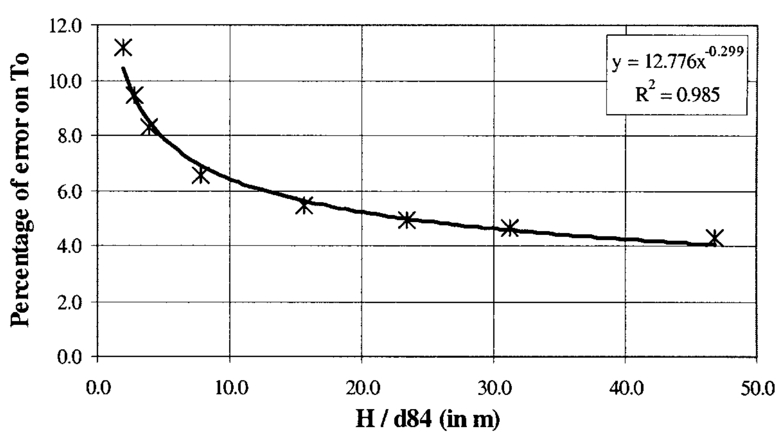

Figure 8. Percentage of error in τ_o due to d_{84} uncertainty within the visual characterization technique and the relationship with depth (H)

Spatially interpolated maps of the three percentiles of the grain sizes distribution (d_{16}, d_{50} and d_{84}) can yield useful insight into several geomorphologic, hydrologic or biologic factors. Analysis of these factors will be improved considerably, because of the ability to take into account the sediment variability within the reach. With the development of the two- and three-dimensional hydrodynamic modelling of river environment, the importance of characterizing the spatial variability of sediment size parameters at the reach scale becomes a major issue.

ACKNOWLEDGEMENTS

Funding for this project was provided by the Natural Sciences and Engineering Research Council of Canada (Collaborative Special Projects), the Fondation de la Faune du Québec, the Government of Québec (Ministère de l'Environnement et de la faune), Government of Canada (Economic development) and the financial partners of CIRSA Inc. (Corporation de soutien aux initiatives de recherche sur le saumon Atlantique). The authors are indebted to the many students coming from McGill University, Montreal University and Sherbrooke University who worked on the collection of the data.

REFERENCES

Adams J. 1979. Gravel Size Analysis from Photographs. *Journal of Hydraulics Division* **105**: 1247–1255.

Bray DI. 1979. Estimating average velocity in gravel-bed rivers. *Journal of Hydraulics Division* **105**(HY9): 1103–1122.

Buffington JM, Montgomery DR. 1999. A procedure for classifying textural facies in gravel-bed rivers. *Water Resources Research* **35**(6): 1903–1914.

Chang HH. 1992. Fluvial Processes in River Engineering. Krieger; Florida.

Church MA, McLean DG, Wolcott JF. 1987. River bed gravel: sampling and analysis. In Sediment Transport in Gravel-bed Rivers, Thorne CR, Bathurst JC, Hey RD (eds). John Wiley & Sons: Chichester; 43–88.

Devries P. 1997. Riverine salmonid egg burial depths: review of published data and implications for scour studies. *Canadian Journal of Fisheries and Aquatic Sciences* **54**: 1685–1698.

Dingman SL. 1984. Fluvial Hydrology. W.H. Freeman and Company; New York.

Einstein HA. 1950. The bedload function for sediment transportation in open channels. US Department of Agriculture and Soil Conservation Service, Technical Bulletin 1026.

Ettema R. 1984. Sampling armor-layer sediments. *Journal of Hydraulics Division* **110**(7): 992–996.

Heggenes J. 1996. Habitat selection by Brown trout (Salmo trutta) and young Atlantic salmon (S. Salar) in streams: static and dynamic hydraulic modelling. *Regulated Rivers: Research & Management* **12**: 155–169.

Heggenes J, Saltveit SJ, Lingaas O. 1996. Predicting fish habitat use to changes in water flow: modelling critical minimum flows for Atlantic salmon, Salmo Salar, and Brown trout, S. trutta. *Regulated Rivers: Research & Management* **12**: 331–344.

Hey RD. 1979. Flow resistance in gravel-bed rivers. *Journal of Hydraulics Division* **105**(HY4): 365–379.

Hoey TB, Ferguson RI. 1994. Numerical simulation of downstream fining by selective transport in gravel-bed rivers: model development and illustration. *Water Resources Research* **30**(7): 2251–2260.

Inman DL. 1952. Measures for describing the size distribution of sediments. *Journal of Sedimentary Petrology* **22**(3): 125–145.

Ippen AT, Drinker PA. 1962. Boundary shear stresses in curved trapezoidal channels. *Journal of the Hydraulics Division* **88**(HY5): 143–179.

Kellerhals R, Bray DI. 1971. Sampling procedures for coarse fluvial sediments. *Journal of the Hydraulics Division* **97**: 1165–1179.

Kondolf GM, Wolman MG. 1993. The sizes of salmonid spawning gravels. *Water Resources Research* **29**(7): 2275–2285.

Koster EH, Rust BR, Gendzwill DJ. 1980. The ellipsoidal form of clasts with practical applications to fabric and size analyses of fluvial gravels. *Canadian Journal of Earth and Sciences* **17**: 1725–1739.

Lane EW, Carlson EJ. 1953. Some factors affecting the stability of canals constructed in course granular materials. Proceedings of the Fifth Congress of the International Association for Hydraulic Research, Minneapolis, Minnesota, September 1–4. 37–48.

Limerinos JT. 1970. Determination of the manning coefficient from measured bed roughness in natural channels. US Geological Survey Water-Supply, Paper 1898-B.

Lisle TE, Madej MA. 1992. Spatial variation in armoring in a channel with sediment supply. In Dynamics of Gravel-bed Rivers, Billi P, Hey RD, Thorne CR, Tacconi P (eds). John Wiley & Sons: Chichester; 277–293.

Marcus WA, Ladd SC, Stoughton JA, Stock JW. 1995. Pebble counts and the role of user-dependant bias in documenting sediment size distribution. *Water Resources Research* **31**(10): 2625–2631.

Mark DM, Church M. 1977. On the misuse of regression in earth science. *Mathematical Geology* **9**(1): 63–75.

McNeil WJ, Ahnell W. 1964. Success of pink salmon spawning relative to size of spawning bed material. US Fish and Wildlife Service Special Scientific Report; Fisheries 469.

Meyer-Peter E, Muller R. 1948. Formulas for Bed-Load Transport. Paper No. 2, *Proceedings of the Second Meeting*. IAHR; 39–64.

Milne JA. 1982. Bed-material size and the riffle-pool sequence. *Sedimentology* **29**: 267–278.

Moir H, Soulsby C, Youngson A. 1996. Geomorphological and hydraulic controls on Atlantic salmon spawning habitat in a tributary of

the River Dee, Scotland. In Proceedings of the second IAHR Symposium on Habitats Hydraulics, Ecohydraulics 2000, Leclerc M, et al. (eds). INRS-Eau: Québec; B3–B14.
Morantz DL, Sweeney RK, Shirvell CS, Longard DA. 1987. Selection of microhabitat in summer by juvenile Atlantic salmon (Salmo salar). *Canadian Journal of Fisheries and Aquatic Science* **44**: 120–129.
Mosley MP, Tindale DS. 1985. Sediment variability and bed material sampling in gravel-bed rivers. *Earth Surface Processes and Landforms* **10**: 465–482.
Muotka T, Petäys AM, Kreivi P. 1996. Spatial relations between lotic fishes, benthic macroinvertebrates and the stream habitat: toward a GIS-assisted approach. In Proceedings of the second IAHR Symposium on Habitats Hydraulics, Ecohydraulics 2000, Leclerc M, et al.: (eds). INRS-Eau: Québec; B45–B54.
Payne BA, Lapointe MF. 1997. Channel morphology and lateral stability: effects on distribution of spawning and rearing habitat for Atlantic salmon in a wandering cobble-bed river. *Canadian Journal of Fisheries and Aquatic Sciences* **54**(11): 2627–2636.
Parker G. 1990. Surface-based bedload transport relation for gravel rivers. *Journal of Hydraulic Research* **28**(4): 417–436.
Richards KS. 1982. Rivers: Form and Process in Alluvial Channels. Methuen: New York.
Rood K, Church MA. 1994. Modified freeze-core technique for sampling the permanently wetted streambed. *North American Journal of Fisheries and Management* **14**: 852–861.
Scherrer B. 1984. Biostatistique. Gaëtan morin éditeur: Chicoutimi.
Sear DA. 1996. Sediment transport processes in pool-riffle sequences. *Earth Surface Processes and Landforms* **21**: 241–262.
Simons DB, Sentürk F. 1992. Sediment Transport Technology. Water and Sediment Dynamics. Water Resources Publications: Colorado.
Sokal RR, Rohlf FJ. 1981. Biometry (second edition). W.H. Freeman and Company: New York.
Walkotten WJ. 1973. A improved technique for freezing-sampling streambed sediments. USDA, Forest Service Pacific Northwest Forest and Range Experiment Station: Portland, Oregon. Research Note PNW-281.
Wentworth CK. 1922. A scale of grade and class terms for clastic sediments. *Journal of Geology* **30**: 377–392.
Whiting PJ, Dietrich WE. 1990. Boundary shear stress and roughness over mobile alluvial beds. *Journal of Hydraulic Engineering* **116**(12): 1495–1511.
Wiberg PL, Smith JD. 1991. Velocity distribution and bed roughness in steep streams, *Water Resources Research* **27**(5): 825–838.
Wilcock PR. 1996. Estimating local bed shear stress from velocity observations. *Water Resources Research* **32**(11): 3361–3366.
Wohl EE, Anthony DJ, Madsen SW, Thompson DM. 1996. A comparison of surface sampling methods for coarse fluvial sediments. *Water Resources Research* **32**(10): 3219–3226.
Wolman MG. 1954. A method of sampling coarse river-bed material. *Transactions of the American Geophysical Union* **35**(6): 951–956.
Zar JH. 1984. Biostatistical Analysis (second edition). Prentice Hall: New Jersey.

